COBEM 2023 27TH INTERNATIONAL CONGRESS OF MECHANICAL ENGINEERING

ABCM Brazilian Society of Mechanical Sciences and Engineering
27th ABCM International Congress of Mechanical Engineering
December 04-08, 2023, Florianópolis-SC, Brazil

COB-2023-0760
A NUMERICAL STUDY OF HEAT AND MASS TRANSFER OF WATER DROPLETS USING DIFFERENT GEOMETRICAL PARAMETERS

Diego Alexandre Agostini
Iago Lessa de Oliveira
Vicente Luiz Scalon
Dep. Engenharia Mecânica/Faculdade de Engenharia - UNESP/Campus de Bauru
d.agostini@unesp.br, iago.oliveira@unesp.br, vicente.scalon@unesp.br

Abstract. *Humidification and dehumidification processes have a wide range of applications in various Engineering equipment. Cooling towers, for example, are equipment widely used in multiple systems to remove high rates of heat generated in processes such as nuclear reactors. Recently, similar devices have emerged that use desiccant liquids to remove moisture from the air stream. This type of device has relevant applications in the pharmaceutical industry and air conditioning systems. Considering the relevance of these various devices presented above, this study proposes to develop a numerical model capable of evaluating the conditions of droplet mass transfer. This assessment depends on a series of geometric and constructive characteristics of the equipment's liquid diffuser. The evaluation is done for different geometric conditions using the OpenFOAM numerical code. The OpenFOAM computational code has no changes implemented, and the mass transfer coefficient is obtained from the mass and energy transport equations analogy. Different droplet spacing and airflow results are evaluated numerically, and the Sherwood Number (Sh) is estimated as the mass transfer coefficient for these conditions. The results provide subsidies for cooling tower systems design according to the type and number of droplets generated. Other studies for the vapor pressure on the surface of desiccant substances also allow generalizing these studies to applications in desiccant liquids systems. Newer studies with new droplet sizes are very important to complement this work.*

Keywords: *Numerical simulation, Heat and mass transfer, Dehumidification, Cooling Tower, OpenFOAM*

1. INTRODUCTION

Cooling technology through evaporative systems have developed significantly during the Industrial Revolution and the development of power cycles. At that time, compact devices capable of cooling large gas flow using a water counterflow were designed. This kind of device has high efficiency because combines the effects of heat and mass transfer and it was known as a cooling tower. Even today, those devices are widely used in large-scale applications in power systems. Nuclear power plants are common examples of the application of cooling towers as the condensing unit of the power cycle.

In the operation of cooling towers, the evaporation processes occurring is of particular importance and was subject of investigations to assess how the overall process could be improved. Bedekar *et al.* (1998), for example, experimentally investigated the filling cooling towers with different air-to-water flow ratios. Recent works on the subject have also been carried out either by experimental techniques or by thermodynamic modeling (Naik *et al.*, 2017; Aadhithiyan *et al.*, 2021). However, more recently numerical simulations, through Computational Fluid Dynamics (CFD), have also been employed in investigations that were concerned with how the phenomenon occurs (Fouda and Melikyan, 2011; Montazeri *et al.*, 2015; Tan *et al.*, 2021; Adam *et al.*, 2022).

More recently, the use of similar principles for liquid desiccant systems has also become relevant. Although desiccant systems have various applications, their most common use has been in air conditioning systems. Both liquid desiccant and humidification systems use dripping or shower mechanisms to carry out their process (Lu *et al.*, 2019; Oladosu *et al.*, 2023; Long *et al.*, 2022).

In this context, this study aims at analyzing the heat and mass transfer on water droplets for application in air-flow humidification devices. We performed CFD simulations of the air flow around the model of a standardized droplet geometry and calculated the drag coefficient and heat and mass transfer coefficients under typical conditions. We also assessed the influence of the relative speed of the droplet to the air on the heat and mass transfer processes.

2. METHODOLGY

Based on the above considerations, this work proposes a numerical model to estimate the heat and mass transfer of a established droplet model.

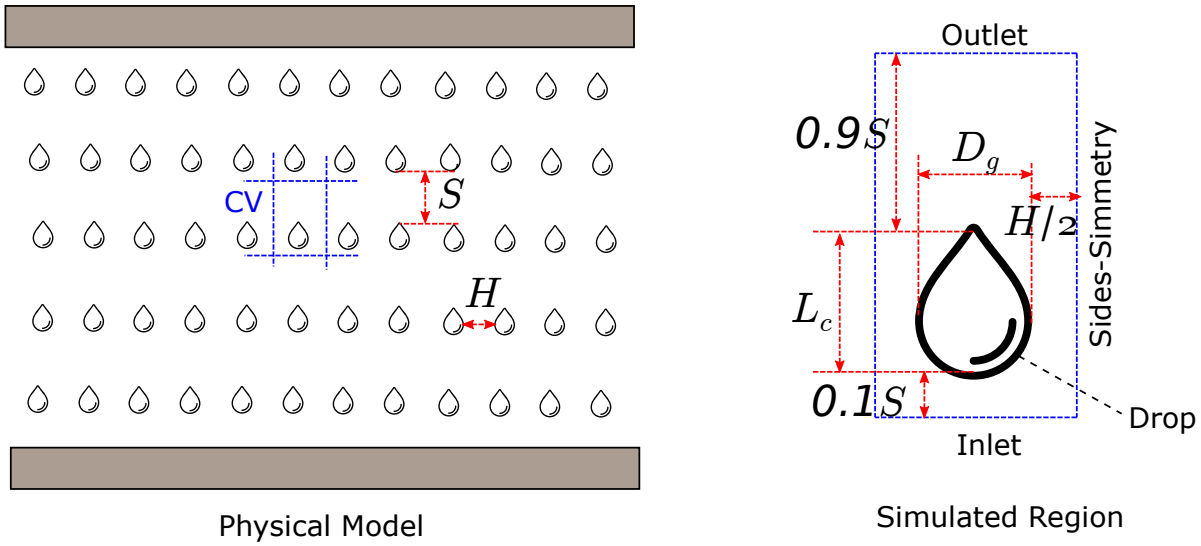

Figure 1. Physical scheme and numerical domain of the modeling

2.1 Numerical Methodology

2.1.1 Physical and Mathematical Modeling

We assumed an incompressible laminar flow of humid air around a droplet, with negligible body forces field and thrust effects. Hence, the continuity and momentum equations for the incompressible flow around a droplet model were solved for the velocity, $\vec{v}$, and pressure, p, fields, given, respectively, by:

$$\frac{\partial \rho}{\partial t} + \nabla \cdot (\rho \mathbf{u}) = 0$$

$$\rho \left(\frac{\partial \mathbf{u}}{\partial t} + \mathbf{u} \cdot \nabla \mathbf{u} \right) = -\nabla p + \nabla \cdot (\mu \nabla \mathbf{u}) + \rho \mathbf{g}$$

Additionally, the energy and mass transport were also solved to account for the thermal and mass transport problems, which were assumed as governed by the general transient-advection-diffusion transport equation for a property ϕ, ss follows:

$$\left(\frac{\partial \phi}{\partial t} + \mathbf{u} \cdot \nabla \phi \right) = \alpha \, \nabla \, (\nabla \cdot \phi)$$

where ϕ represent either the humidity concentration and the temperature fields and, moreover, the equations are differentiated by the boundary conditions and by the thermal or mass diffusivity values, as follows:

- thermal problem: $\phi = T$, $\alpha = \alpha_T = k/(\rho \, c_p)$;
- mass transfer problem: $\phi = \rho^*$ (concentration), $\alpha = \alpha_m = D_{A,B}$;

For the thermal problem, it is important to note that no energy generation effects were assumed and the viscous dissipation was considered negligible. Additionally, we also assumed that the droplet volume remains constant during the process and that the disturbed wake in the droplet rear flow do not affect the flow on the sibsequente droplet.

2.1.2 Geometry and Boundary Conditions

We assumed a three-dimensional modeling of a droplet. Rigourously, the problem at hand typically involves several drops that are moving side by side and sequentially, thus, when considering a single droplet, all lateral surfaces can be treated as symmetry planes (see Figure (1), left panel, for a schematic representation of the described modeling and its right panel for a description of the geometry and boundary conditions assumed). At the front of the droplet, an inlet condition was applied with a uniform velocity profile and at the outlet the pressure was assumed zero with a local-parabolic condition for the velocity field. Finally, on the droplet surface we assumed the no-slip velocity condition.

For the thermal and mass transport governing equations, we assumed the following boundary condtions:

- At the inlet: $T = T_\infty$, $\rho^* = \rho^*_\infty$;

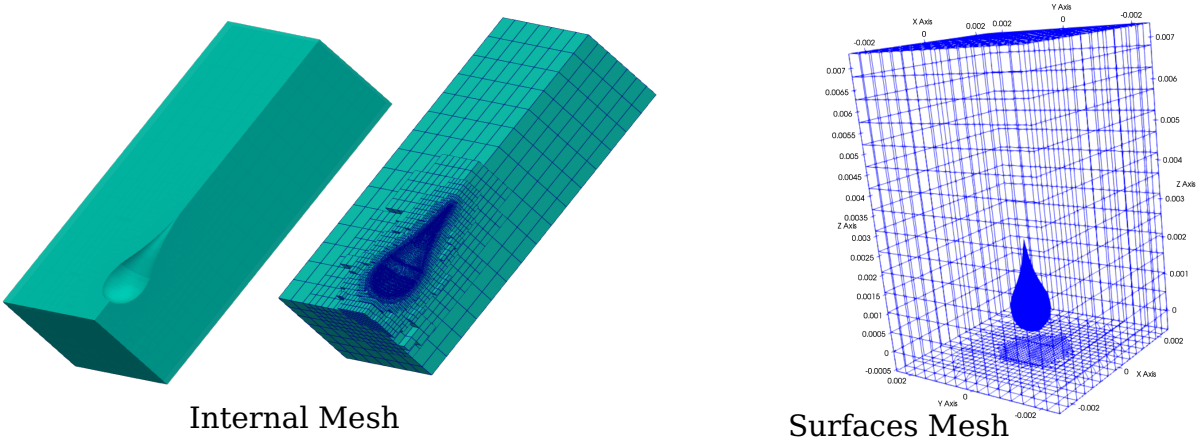

Figure 2. Problem mesh generated using *snappyHexMesh*.

- At the outlet and symmetry planes: $\partial T/\partial \mathbf{n} = 0$, $\partial \rho^*/\partial \mathbf{n} = 0$;
- Droplet surface: $T = T_s$, $\rho^* = \rho_s^*$;

2.1.3 Numerical Method

The presented physical model was solved in OpenFOAM code using the solvers *simpleFoam*, for the fluid flow, and *scalarTransportFoam*, for the energy and mass transport governing equations. With the velocity and temperature/mass fractions fields, we computed the heat and mass transfer coefficients under the given conditions conditions.

The main drop geometric parameters are the maximum diameter $D_g = 1$ mm and total length $L_c = 2.47$ mm. Other drop physical parameters were estimated from the **STL** file using MeshLab software. Based on this process, several unknown characteristics could be measured, such as the drop volume $V_g = 0.77745$ mm³ and its surface area for heat and mass exchange $A_{sg} = 4.5383$ mm².

The problem mesh was generated using an OpenFOAM script (*snappyHexMesh*), created from a **STL** type file assembled for the drop. The result generates a very fine mesh close to its surface that includes boundary layer elements. A section of the problem domain to show the generated mesh can be seen at Figure 2. A refinement close to the surface was used to ensure the accuracy of the obtained results.

2.1.4 Data Analysis

In the case of the thermal problem, the value of the Nusselt number can be determined from the temperature gradient on a defined surface, so that:

$$\text{Nu} = \frac{h\,L_c}{k} = \frac{L_c}{T_s - T_\infty}\left.\frac{\partial T}{\partial \mathbf{n}}\right|_{\text{surf}}$$

and, on the other hand, for the mass transfer problem the Sherwood number can be obtained by:

$$\text{Sh} = \frac{h^*\,L_c}{D_{A,B}} = \frac{L_c}{\rho_s^* - \rho_\infty^*}\left.\frac{\partial \rho^*}{\partial \mathbf{n}}\right|_{\text{surf}}$$

By using these dimensionless parameters, we evaluated the rates of heat transfer and evaporation on the surface of the drop.

Furthermore, the terminal velocity is another important parameter to consider in this study and can be defined as the speed when weight and drag forces are balanced. Considering this situation, the terminal velocity of the droplet U_g can be calculated as follows:

$$U_g = \sqrt{\frac{2\,g\,\rho_w\,V_g}{A_{fg}\,C_D\,\rho_a}}$$

where g is the local gravity acceleration; ρ_w and ρ_a are the specific masses of water and air, respectively; C_D is the drag coefficient of the drop, V_g is the volume of the droplet and A_{fg} is the frontal area of the drop, calculated based on the maximum diameter of the drop D_g.

The application of these principles allows to identify the behavior of velocities and temperature or concentrations profiles and their influence on the average and local heat and mass transfer rates. The study presents some results for the

variation of the velocity U and Reynolds number of the drop (Re=$U\ L_c/\nu$). For the case studied, the physical properties will be assumed as average values for air (Pr= 0.79) and the diffusion of water in air (Sc= 0.8). We evaluated the following parameters: the drag coefficient (C_D), which allows the determination of the velocity limit of the drop (U_d), as explained previously; additionally, considering that the total velocity of the drop was simulated, the complement of the limit velocity up to the total value is the ascending airflow velocity (U_a); finally, we computed the average Nusselt number, to evaluate the heat transfer, by numerically integrating of the results of the temperature gradients in their normal direction over the entire surface of the drop.

The initial formulation treated this problem as a laminar flow. However several vortices was formed at the back region of the drop. Therefore, it was necessary to use a model to treat the effects of turbulence in the surface surroudings. In this study, the Spalart–Allmaras model was chosen as it is usually indicated in cases where an external flow is studied. This model is included in the *Reynolds Averaged Simulation (RAS)* class and has a statistical treatment of the turbulence terms to define a turbulent viscosity. This method was originally developed by Spalart and Allmaras (1992) for aerospace simulations with calibrated parameters for accurated separation flows treatment. Details of the implemented model can be seen at Greenshields (2023).

3. RESULTS AND DISCUSSIONS

Figure 3 shows the velocity magnitude field. In this figure, we can note the formation of recirculating zones, from the point where the narrowing of the drop begins, which is a consequence of a low-pressure region. Despite this effect, one can see that the wake formed was short, mainly if compared to that of cylinders, and closed shortly after the drop's end tip. Small disturbances in the posterior region remain up to the outlet.

The temperature profile inside the studied region can be seen in Figure 4 for the different inlet velocities. The presented

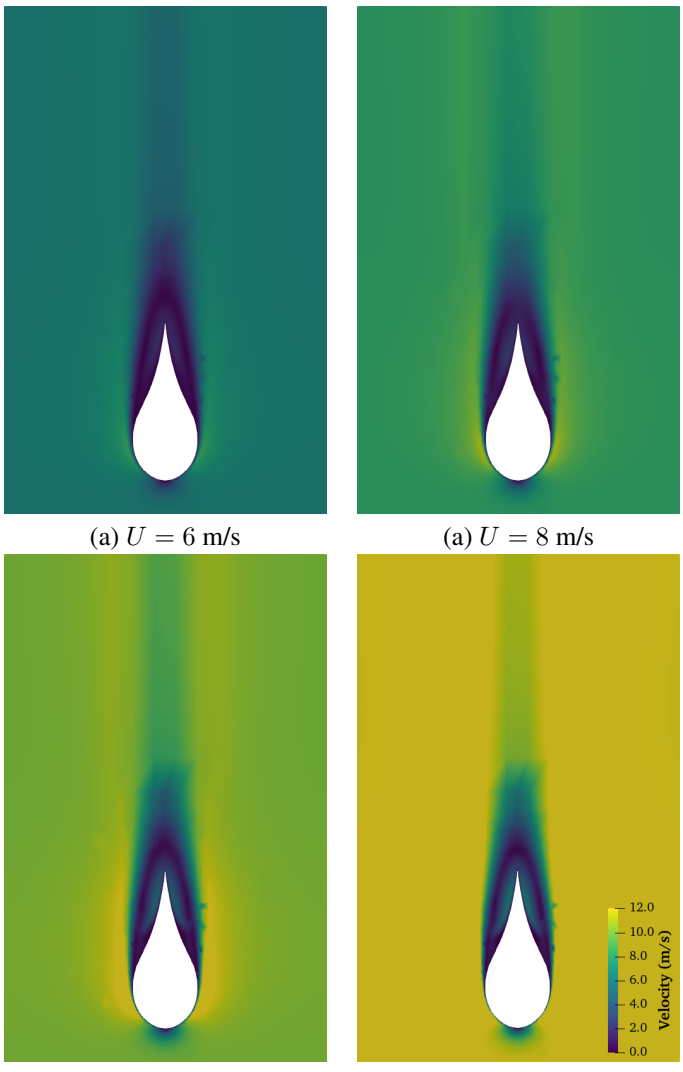

(a) $U = 6$ m/s (a) $U = 8$ m/s

(c) $U = 10$ m/s (a) $U = 12$ m/s

Figure 3. Air velocity around the droplet for the inlet velocity range tested.

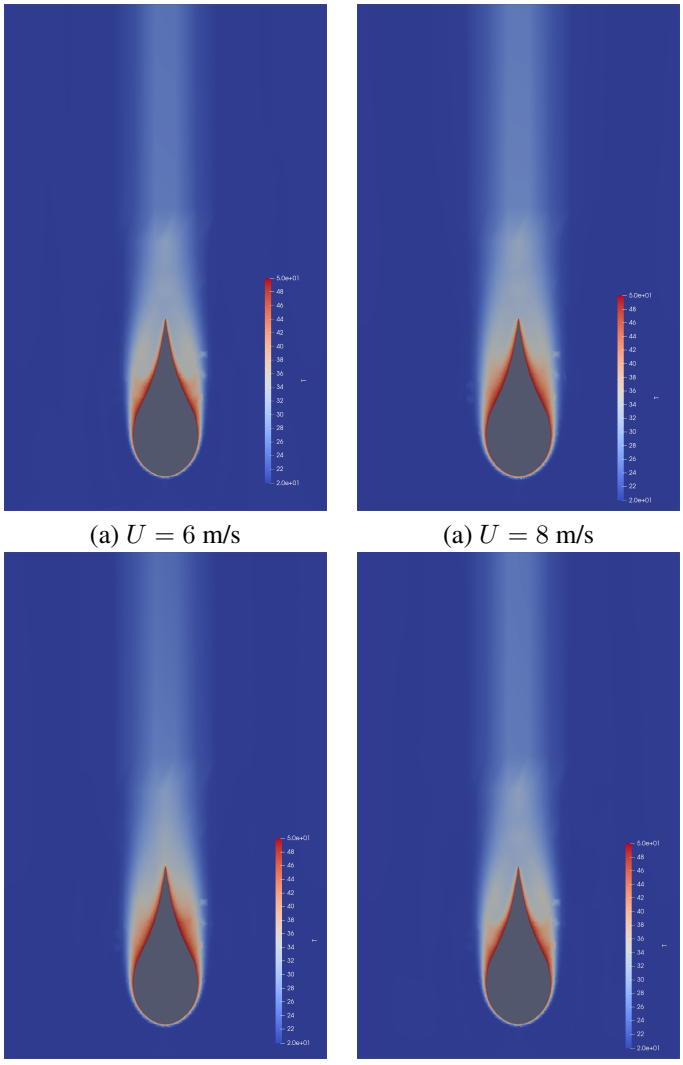

(a) $U = 6$ m/s (a) $U = 8$ m/s

(c) $U = 10$ m/s (a) $U = 12$ m/s

Figure 4. Air temperature fields for the range of inlet velocities

results also show an affected region of a thin boundary layer around the droplet. There is a larger growth of this disturbed region only in the narrowing region of the droplet, agreeing with the previously highlighted low-pressure region. Small differences in these fields can be noted between different free-stream conditions.

We can see that in both the velocity and temperature fields there is a disturbance propagation in the back region of the drop up to the outlet zone. This condition may affect one of our hypotheses suggesting that flow would be undisturbed right at the next drop. To better quantify the level of this disturbance, we evaluated the behavior of the velocity field in the central line of the flow outlet (shown in Fig. 5). We can see that there is a small disturbance in the velocity field resulting from the flow around the drop with increasing inlet velocity accentuating this disturbance. Nevertheless, the disturbance it not pronounced for this drop spacing, and a more detailed study on the subject should be carried out in the future.

Table 1 show the physical parameters considered in this study. Although the averaged Nusselt number (Nu_m) is a very important parameter to obtain the total heat transfer of the drop, it is also relevant to know how the local value Nu_l behaves along the drop surface. Figure 6 shows this information along the surface. The figure clearly shows that the value of Nu_l starts a little low at the stagnation point but quickly rises. Thus, the front region of the drop and the end of the rear

Table 1. Physical parameters computed in this study.

U[m/s]	Re	C_D	U_d[m/s]	U_a[m/s]	Nu_m
6	926	0.6616	4.94	1.06	27.97
8	1235	0.6189	5.10	2.90	31.12
10	1544	0.5724	5.31	4.69	34.86
12	1852	0.5522	5.40	6.60	37.77

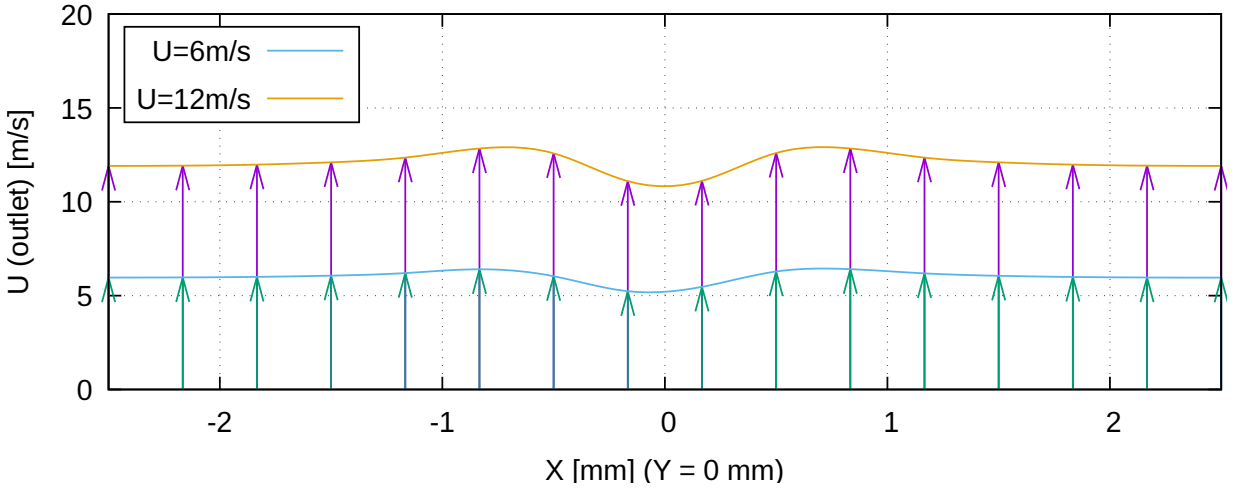

Figure 5. Velocity profile at the outlet of the flow domain.

region are the places where the highest heat transfer is verified. It should be noted, however, that the region of the drop rear tip has a high heat transfer rate, but has a small exposed surface. This combination of effects means that the total heat exchange in this region tends to be very small. As was also predictable, the highest heat transfer rates may occur in the cases with high total velocity conditions.

4. CONCLUSIONS

Considering the results obtained, we can conclude that:

- the droplet terminal velocity is relevant for the evaluation of heat transfer and cannot be ignored when estimating the air velocity resulting from the flow;
- the drop frontal region, next to the stagnation point, is where is verified the largest heat transfer (this effect cannot be perceived in the plot);
- the increase in the total relative velocity implies an increase in the heat transfer rate;
- there is a region at the beginning of droplet strangulation where heat transfer rate is very low. In this region, it was not possible to establish a correlation between the increase in speeds and the increase in Nu_l.
- the velocity perturbation wake, at least in the case with the studied geometry, reaches the outlet domain and, consequently, affects the conditions of the inflow of the next drop.

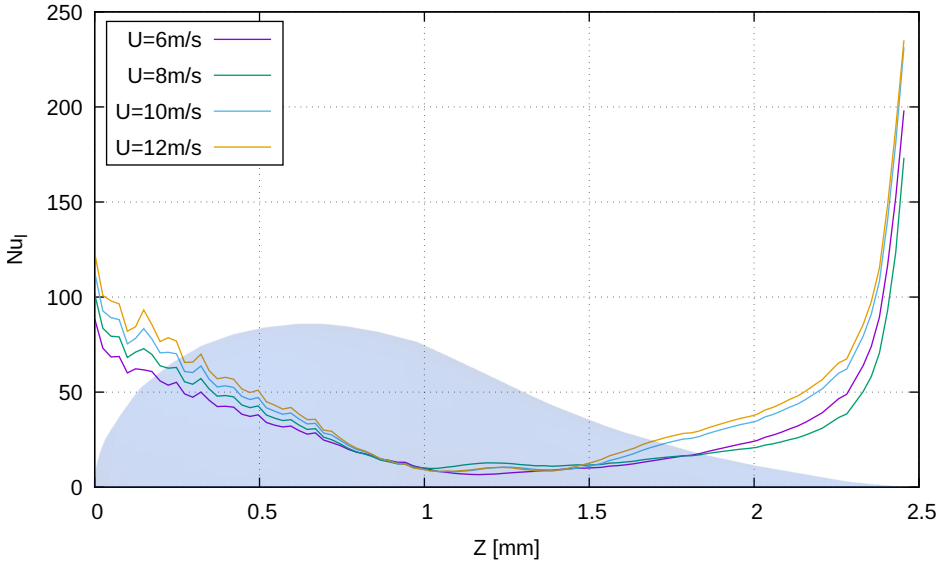

Figure 6. Local behavior of the Nusselt number along the droplet vertical length.

Future works should be developed considering the evaluation of the variation of the drop geometrical parameters. Other results can still be obtained with the development of this work, such as the estimated mass transfer coefficient through the Sherwood number, either local or averaged over the drops area. In addition, possible evaluations of the mesh and eventual comparison with other numerical and experimental results would also contribute to this work. Finally, an analysis of the effects of disturbances in the flow on the subsequent drops should also be carried out.

5. REFERENCES

Aadhithiyan, A., Sreeraj, R., Naik, B.K. and Anbarasu, S., 2021. "Assessment of evaporative cooling process across the mechanically driven cooling tower based on two-point boundary value problem using novel integral technique". *International Journal of Refrigeration*, Vol. 131, pp. 254–262. doi:10.1016/j.ijrefrig.2021.08.002.

Adam, A., Han, D., He, W., Amidpour, M. and Zhong, H., 2022. "Numerical investigation of the heat and mass transfer process within a cross-flow indirect evaporative cooling system for hot and humid climates". *Journal of Building Engineering*, Vol. 45, p. 103499. doi:10.1016/j.jobe.2021.103499.

Bedekar, S., Nithiarasu, P. and Seetharamu, K., 1998. "Experimental investigation of the performance of a counter-flow, packed-bed mechanical cooling tower". *Energy*, Vol. 23, No. 11, pp. 943–947. doi:10.1016/s0360-5442(98)00044-9.

Fouda, A. and Melikyan, Z., 2011. "A simplified model for analysis of heat and mass transfer in a direct evaporative cooler". *Applied Thermal Engineering*, Vol. 31, No. 5, pp. 932–936. doi:10.1016/j.applthermaleng.2010.11.016.

Greenshields, C., 2023. *OpenFOAM v11 User Guide*. The OpenFOAM Foundation, London, UK. URL `https://doc.cfd.direct/openfoam/user-guide-v11`.

Long, T., Zheng, D., Li, Y., Liu, S., Lu, J., Shi, D. and Huang, S., 2022. "Experimental study on liquid desiccant regeneration performance of solar still and natural convective regenerators with/without mixed convection effect generated by solar chimney". *Energy*, Vol. 239, p. 121919. doi:10.1016/j.energy.2021.121919.

Lu, Y., Roskilly, A.P., Huang, R. and Yu, X., 2019. "Study of a novel hybrid refrigeration system for industrial waste heat recovery". *Energy Procedia*, Vol. 158, pp. 2196–2201. doi:10.1016/j.egypro.2019.01.620.

Montazeri, H., Blocken, B. and Hensen, J., 2015. "Evaporative cooling by water spray systems: Cfd simulation, experimental validation and sensitivity analysis". *Building and environment*, Vol. 83, pp. 129–141. doi:10.1016/j.buildenv.2014.03.022.

Naik, B.K., Choudhary, V., Muthukumar, P. and Somayaji, C., 2017. "Performance assessment of a counter flow cooling tower – unique approach". *Energy Procedia*, Vol. 109, pp. 243–252. doi:10.1016/j.egypro.2017.03.056.

Oladosu, T.L., Al-Kayiem, H.H., ul Haq Gilani, S.I., Baheta, A.T. and Horng, T.W., 2023. "Performance enhancement of electrodialysis regeneration of deep eutectic solvent for liquid desiccant air conditioning systems". *Journal of Building Engineering*, Vol. 70, p. 106343. doi:10.1016/j.jobe.2023.106343.

Spalart, P. and Allmaras, S., 1992. "A one-equation turbulence model for aerodynamic flows". doi:10.2514/6.1992-439.

Tan, H., Wen, N. and Ding, Z., 2021. "Numerical study on heat and mass transfer characteristics in a randomly packed air cooling tower for large-scale air separation systems". *International Journal of Heat and Mass Transfer*, Vol. 178, p. 121556. doi:10.1016/j.ijheatmasstransfer.2021.121556.

6. RESPONSIBILITY NOTICE

The following text, properly adapted to the number of authors, must be included in the last section of the paper:
The author(s) is (are) solely responsible for the printed material included in this paper.